Journal of Clinical and Medical Images

Research Article

ISSN: 2640-9615 | Volume 8

Use of Optical Coherence Tomography images to Differentiate Between Normal Skin, Skin Lesions, and Melanoma: A Pilot Study

Frederick H Silver[1,2], Tanmay Deshmukh[2], Hari Nadiminti[3], Cindy Wassef[1,4], Amy Pappert[1,4], Abisola Lawal[1], and Aanal Patel[1]

[1]Department of Pathology and Laboratory Medicine, Robert Wood Johnson Medical School, Rutgers, the State University of New Jersey, Piscataway, NJ 08854, USA

[2]OptoVibronex, LLC., Ben Franklin Tech Ventures, Bethlehem, PA 18105, USA

[3]Summit Health, Dermatology, Berkeley Heights, NJ 07922, USA

[4]Rutgers Center for Dermatology, Somerset, NJ 08873, USA

***Corresponding author:**

Frederick H Silver,
Department of Pathology and Laboratory Medicine, Robert Wood Johnson Medical School, Rutgers, the State University of New Jersey, Piscataway, NJ 08854, USA

Received: 26 Oct 2024
Accepted: 16 Nov 2024
Published: 21 Nov 2024
J Short Name: JCMI

Citation:

Frederick H Silver, Use of Optical Coherence Tomography images to Differentiate Between Normal Skin, Skin Lesions, and Melanoma: A Pilot Study. J Clin Med Img. 2024; V8(6): 1-11

1. Abstract

Optical coherence tomography is a technique used extensively in ophthalmology to diagnose several ocular diseases. It is being used in dermatology to diagnose skin conditions. We are developing a technique termed vibrational optical coherence tomography (VOCT) to noninvasively image (OCT) and measure the physical properties of tissue components using vibrational analysis in biopsies of skin lesions. In this study we analyze OCT images by subdividing them by pixel intensity differences. OCT images are broken down into green (low pixel intensity), blue (medium pixel intensity), and red (high pixel intensity) images using a fire look-up table. It is demonstrated using this approach that images of normal skin and skin lesions are quite different. The results of this pilot study suggest that this approach may provide information to differentiate benign from cancerous lesions noninvasively. Additional studies are needed to quantitatively analyze these images and to compare the results to the results of vibrational measurements that have been reported previously.

2. Introduction

Optical coherence tomography (OCT) is an interferometric technique using a low coherence infrared light source, which allows light to penetrate skin without causing tissue changes [1, 2]. OCT has been used in ophthalmology to help diagnose and manage many eye conditions including glaucoma, diabetes related retinopathy, macular degeneration, ocular tumors, and vitreous conditions [3]. It is also used in dermatology for evaluation of benign and cancerous lesions [1, 2]. OCT uses infrared light reflected from the different components of surface tissues to generate an image. It provides cross-sectional and en face images of skin at depths between 0.4 and 2.0 mm with resolution between 3 and 15 micrometers [1]. Dermatologic clinical applications include detection of nonmelanoma skin cancer such as basal cell carcinoma, abnormal vasculature, evaluation of therapy for inflammatory and connective tissue diseases [1, 2]. It also has been reported to be used to evaluate malignant melanoma, skin infestation, bullous diseases, tattoos, nails, hemangiomas, diabetic foot ulcers, psoriasis, atopic dermatitis, and basal cell and squamous cell carcinomas [4-8]. Epidermal thickness changes measured using OCT are associated with several diseases [6-8]. Collagen content in normal skin and fibrotic skin diseases including systemic sclerosis and hypertrophic scars secondary to burn, trauma, and other injury can be analyzed using OCT images [9, 10]. The results of studies on skin led to the observation that OCT imaging has the potential to

serve as an objective, non-invasive measure of collagen's status and disease progression for use in both research trials and clinical practice [10].

OCT provides quick and useful diagnostic images for several clinical problems and is a valuable addition or complement to other noninvasive imaging tools such as dermoscopy, high-frequency ultrasound, and confocal laser scanning microscopy [11]. While OCT images alone are useful for visual interpretation of skin lesions, there is more quantitative information that can be deduced from the images such pixel intensity differences between normal skin and skin lesions [12]. Complete interpretation of OCT images requires an understanding of the basis of interaction of light with skin.

Light propagation and penetration through tissues is dependent on reflection, scattering, and absorption by the different component layers. Only approximately 4–7% of visible light is reflected by the skin surface, regardless of incident wavelength, pigmentation, or structure [13]. This means that most of the light contacting the skin surface penetrates through the stratum corneum and enters the epidermis and dermis [13]. The remainder of the light is then either absorbed or scattered. Keratins, collagen, melanin, and hemoglobin are the primary skin molecules responsible for the visible light penetration via scattering and absorption [13]. Epidermal scattering of light entering the skin can be greater due to melanin in the epidermis especially for large aggregates [13,14]. In normal skin the scattering due to small melanin particles, Rayleigh scattering, occurs in all directions if the particle size is less than the wavelength of the light divided by about 10 [13, 14]. Mia scattering in the forward direction (along the beam direction) occurs when the diameters of the scattering elements such as melanin, cellular aggregates, and collagen fibers are near the light wavelength [13, 14]. The primary chromophores in skin, melanin, heme, and opsin photoreceptors provide little absorption of light between light wavelengths of 600 and 1300 nm [15-17]. Melanin absorption occurs in the UV light spectrum and decreases in the visible light and infrared spectra [15-17]. The ability of melanin to absorb ultraviolet light with wavelengths between 100 and 400 nm protects skin from UV light damage. Two forms of melanin exist in skin, eumelanin and pheomelanin [18]. Eumelanin creates a black-brown color in skin, photoprotecting skin by transducing radiation energy into heat [19]. Since the beneficial effects of melanin are attributed mainly to eumelanin, it has been proposed that skin cancer is due to the reduced eumelanin in the skin and increased formation of pheomelanin [20]. Therefore, the scattering potential for melanin in the skin may be different in normal skin and benign skin lesions when compared to melanomas due to differences in the melanin particle sizes and types. Results of previous studies using vibrational OCT illustrate that the scattering of light at 840 nm by melanomas containing small and large lesions is different from that of normal skin based on pixel intensity versus depth plots [12]. The purpose of this paper is to study OCT images based on pixel intensity differences of normal skin and different skin cancers to identify whether melanin scattering differences between normal skin, melanomas, and other skin cancers may be useful in identifying the differences between benign and cancerous lesions. In this study we begin to compare differences between OCT images of seborrheic keratoses, a benign pigmented lesion, with melanoma, a pigmented lesion as an example of how use of pixel intensity measurements may be useful identifying the differences between benign and cancerous lesions noninvasively.

3. Methods

3.1. OCT Image Collection and Measurement of Resonant Frequency

Images of normal skin and skin lesions were collected using an OQ Labscope 2.0 as described previously. The instrument operates at a wavelength of 840 nm and collects images at 13,000 lines per second [12, 21]. Raw image OCT data were collected and processed using MATLAB software and image J [12, 21]. All OCT images were scanned through the lesion cross-section parallel to the surface to create pixel images as reported previously [12, 21]. The pixel intensity across the sample as a function of depth was collected. All images were made from intact skin and biopsies as part of IRB approved clinical studies of 21 subjects with normal skin, 56 of basal cell carcinomas, 53 of squamous cell carcinomas, 46 melanomas and 22 seborrheic keratoses at both Summit Health and Robert Wood Johnson Medical School. OCT images were color-coded for observation based on the pixel intensity at each location within the cross section to enhance image details for visual analysis [12, 21]. The color – coding of the OCT images was done using a lookup table (LUT) "Fire" as described previously [22]. Each pixel value in the grayscale OCT images is assigned a unique combination of Red-Green-Blue values using the LUT (Table 1). By application of digital image processing algorithms on the color – coded OCT image, the images were split into red, green, and blue channels based on the distribution of pixel intensities. Since a combination of red, green, and blue colors in varying intensities can produce all the colors in the color – coded image, the image processing algorithms map the blue, red, and green components of each pixel. By breaking up the total image into differences in pixel intensity distribution at each point, it is possible to examine differences in scattering potential of the different layers of skin and skin lesions. Skin layers containing large aggregates greater than about one tenth of the light wavelength will scatter light in the forward direction and appear to have lower surface pixel intensities compared to normal skin. If large lesion aggregates exist, whether they be due to melanin particles, cell aggregates, or large diameter collagen fibers, they should limit light reflection and result in a decrease in OCT image brightness of the epidermis.

4. Results

4.1. Color-Coded OCT Images

A variety of different subsurface details were observed when the skin lesions were imaged in the OCT scanning mode. These include the stratum corneum, basal epithelium, and the papillary dermis. While individual cells are not visible via conventional OCT, the stratum corneum, basal epithelium, rete pegs, and papillary dermis are seen as described previously [12, 21] (Figure 1A). These layers are easier to observe when the OCT image is color-coded based on the pixel intensity using image J. Figure 1 shows typical color-coded OCT images of typical examples of normal skin (A), basal cell carcinoma (BCC), squamous cell carcinoma (SCC) (C), and melanoma MEL (D). Note normal skin contains an undulating well defined stratum corneum and rete pegs. Nodular BCC contains an interrupted stratum corneum and black nodular spots near where the rete pegs were once located (B), while SCC exhibits a high cellular pixel intensity just below where the stratum corneum is normally present. Figures 2, 3, and 4 show images created from the different pixel intensities generated using Table 1. The green, blue, and red channels that are derived from the images shown in Figure 1 reflect low, medium, and high pixel intensity images. These images illustrate the possible use of pixel intensity data to differentiate between normal skin and cancerous lesions. Note SCC and MEL exhibit lower surface pixel intensities in the green channel image possibly due to the formation of cell aggregates, melanin particles, and fibrotic collagen that scatter light towards the papillary dermis. Figures 5 and 6 show typical images for 5 typical seborrheic keratoses and for 5 typical melanomas obtained from skin biopsies. When the images in Figures 2, 3, and 4 were scanned parallel to the surface of the sample, a pixel intensity versus depth plot is created. The images are separated by pixel intensities using the look up chart shown in Table 1. The lowest pixel intensities were used to generate an image (green channel); the images look quite different as shown in Figure 2. The green channel image is very low for SCC and melanoma suggesting that light is forward scattered from the stratum corneum into deeper layers in these lesions. The pixel intensity of SCC and melanoma are much lower than that of normal skin and BCC. In contrast, the blue channel images for the SCC and MEL are more like that of normal skin as shown in Figure 6. The red channel is much weaker for melanoma than for the other lesions, suggesting MEL may be differentiated from the others skin lesions based on the green and red channels. SCC may also be differentiated from the others based on the green and red channels. When 5 typical images of a cancerous pigmented lesion (melanoma-Figure 5) were compared to 5 pigmented benign lesions (seborrheic keratosis (SK) as shown in Figure 6, it is seen that differences in the pixel intensity of the stratum corneum (yellow color) are seen. The stratum corneum of SK lesions appears much brighter than that of the melanomas. This intensity difference also appears to occur in the green channel images of melanomas (Figure 7) and SK lesions (Figure 8). Differences in the blue channel images are not as evident (Figures 9 and 10) while the intensity of the red channels of melanomas (Figure 11) appear somewhat less than that of the SK.

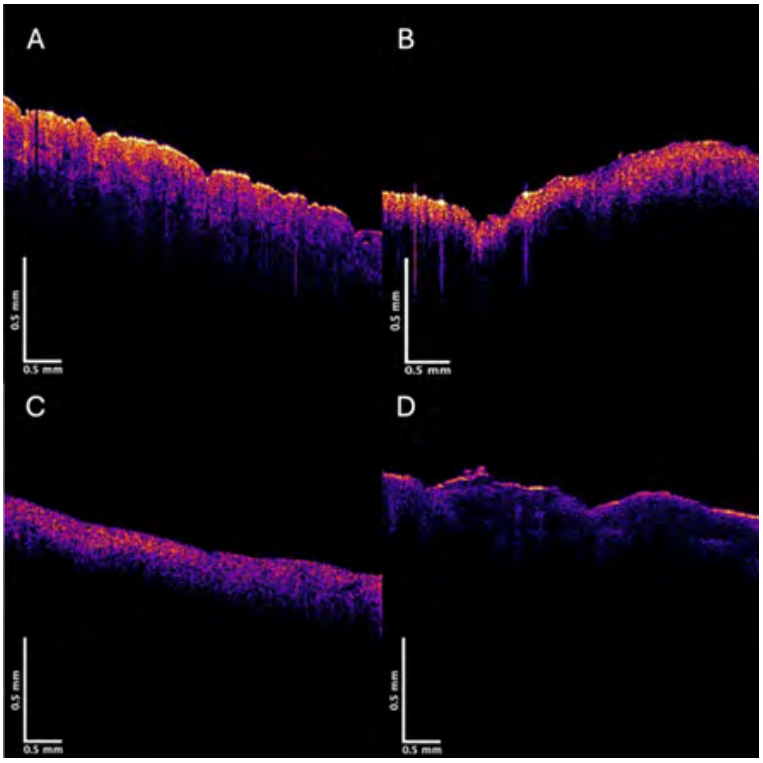

Figure 1: Color-coded OCT images of normal skin (A), basal cell carcinoma (B-BCC), squamous cell carcinoma (C-SCC), and melanoma (MEL-D) obtained by superimposing green, blue, and red pixel intensities on the gray scale image. Note normal skin has a bright yellow stratum corneum, pink and yellow germinative layers, and blue basal and papillary layers.

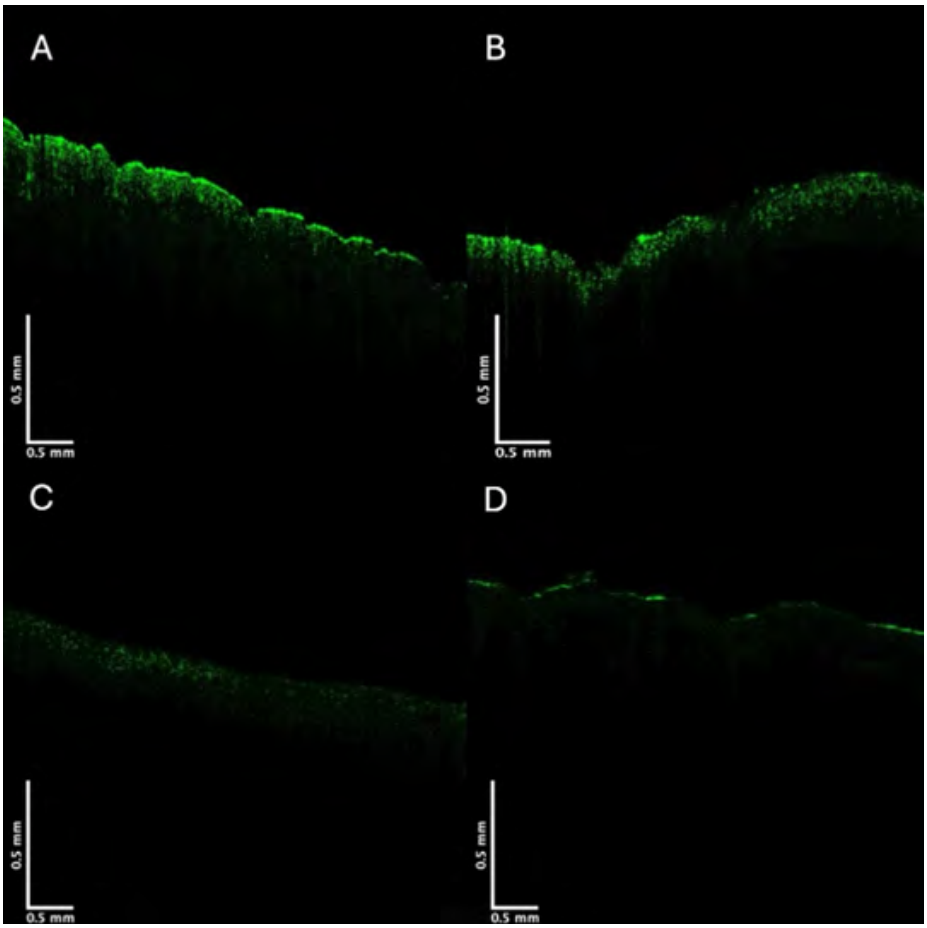

Figure 2: Green channel color-coded OCT low pixel intensity images for normal skin (A), basal cell carcinoma (B), squamous cell carcinoma (C), and melanoma (D) obtained using Table 1. Note green channel images for SCC and MEL have lower pixel intensities compared to BCC and MEL.

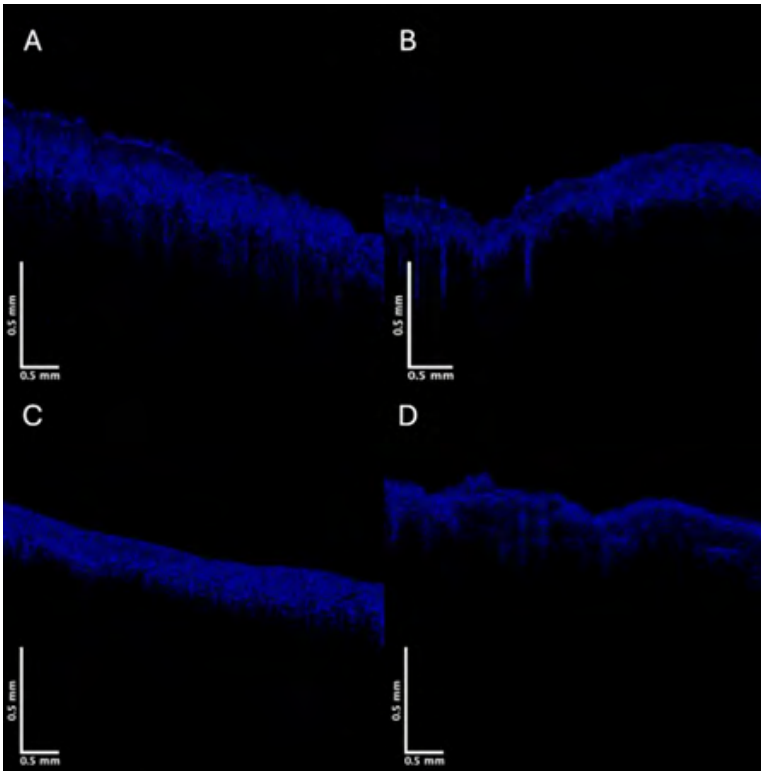

Figure 3: Blue channel (medium pixel intensity) images for normal skin (A), basal cell carcinoma (B), squamous cell carcinoma (C), and melanoma (D). Note blue channel image has a lower pixel intensity for MEL compared to the other images.

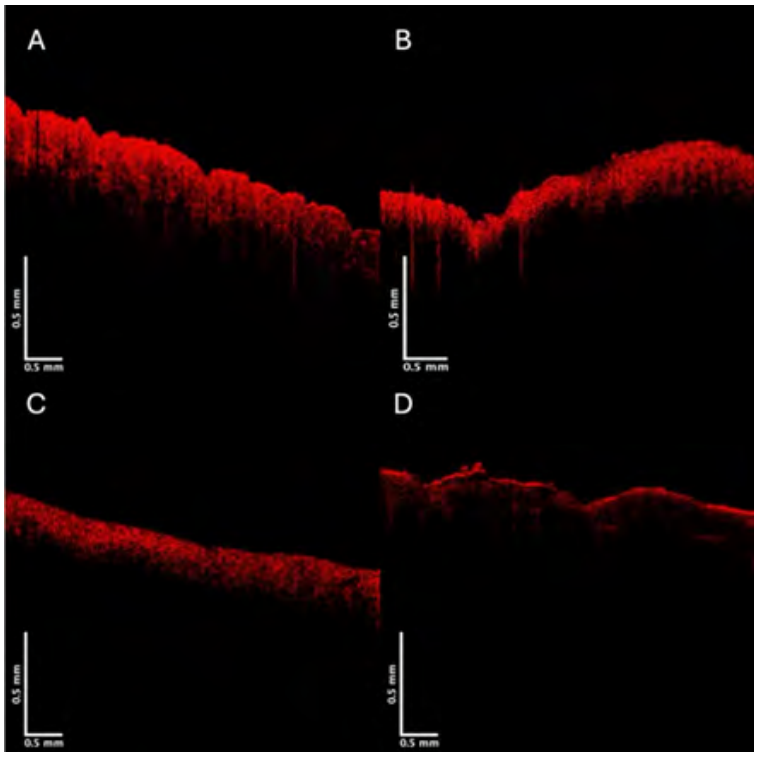

Figure 4: Red channel (high pixel intensity measurements) for normal skin (A), basal cell carcinoma (B), squamous cell carcinoma (C), and melanoma (D). Note the red channel image of melanoma has a lower pixel intensity than that of the other specimen.

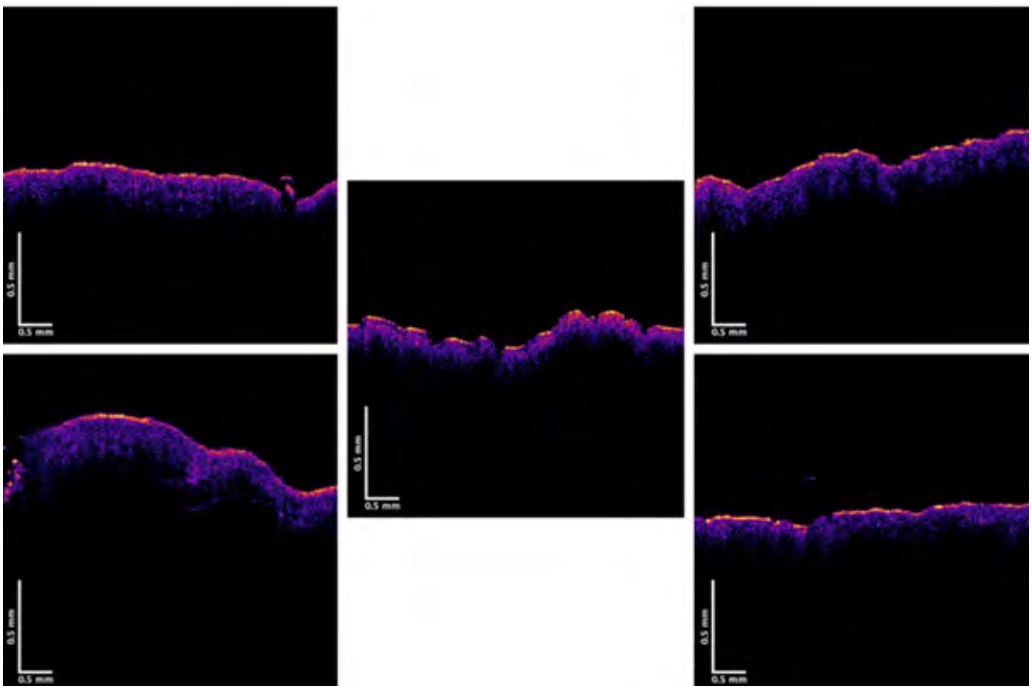

Figure 5: Color-coded OCT images of the cross-section of 5 different melanomas. Note lack of the yellow surface layer from the stratum corneum.

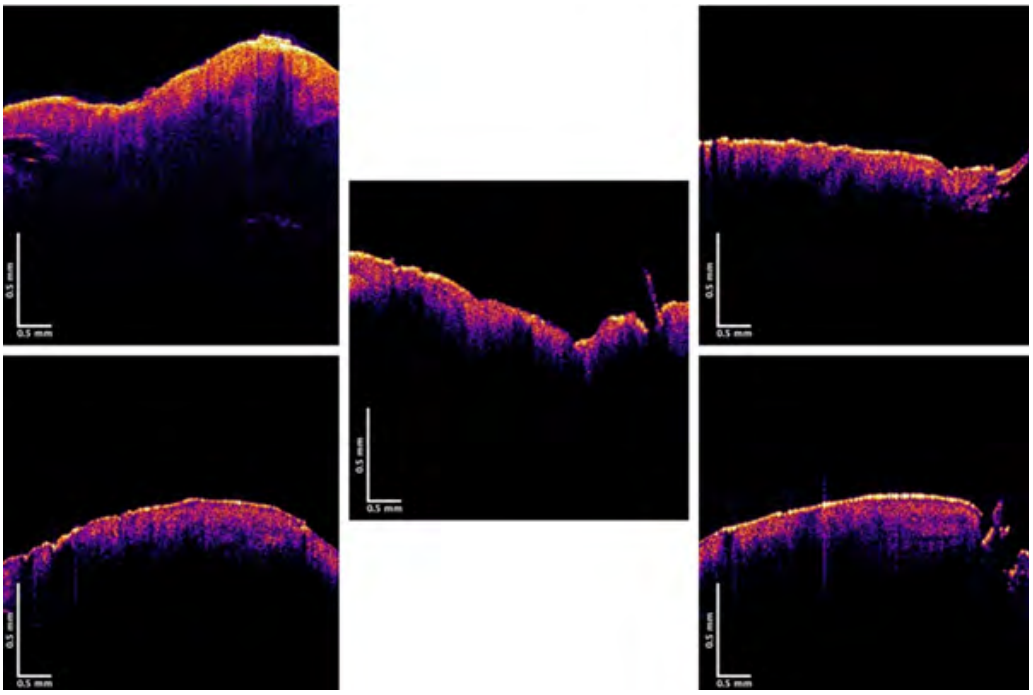

Figure 6: Color-coded OCT images of 5 different seborrheic keratoses. Note the bright yellow surface layer from the stratum corneum.

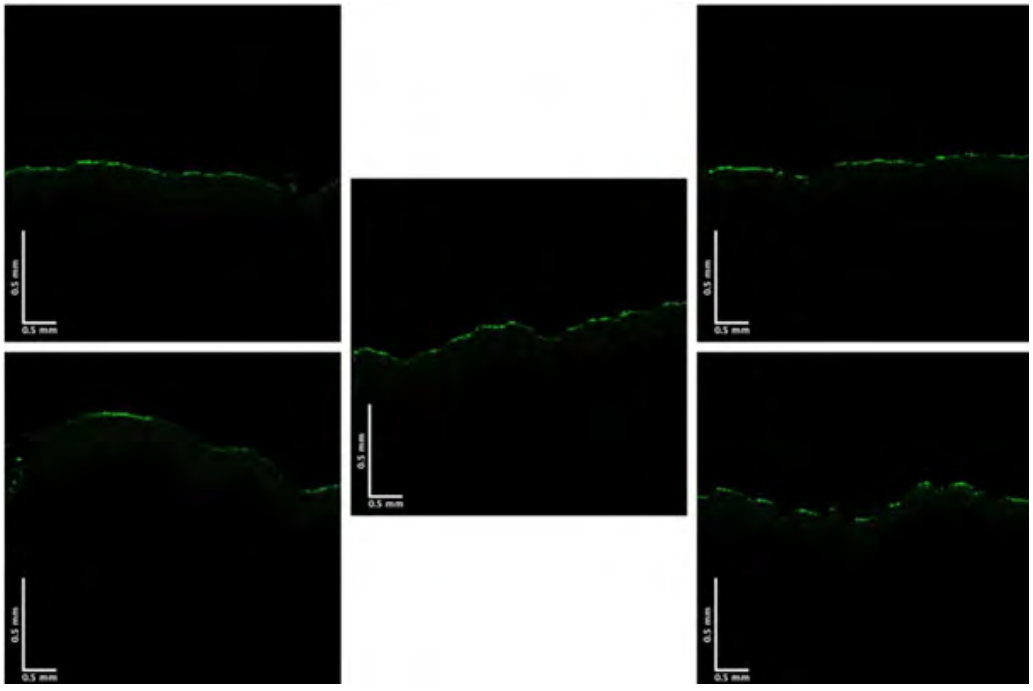

Figure 7: Green channel OCT images for 5 melanomas. Note the lack of pixel intensity of the melanomas.

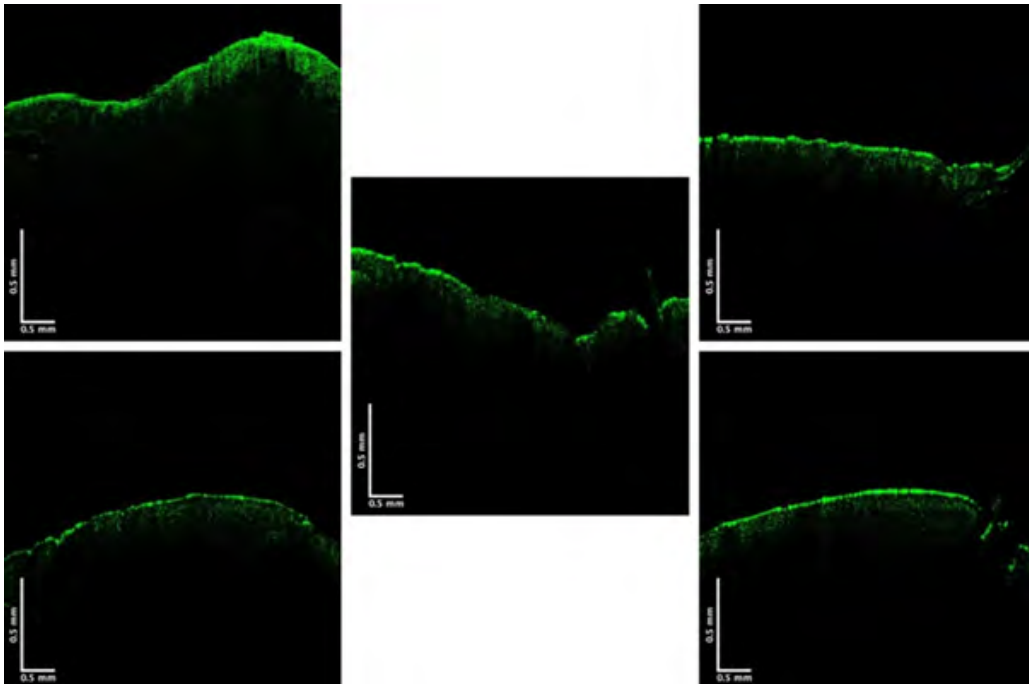

Figure 8: Green channel OCT images for 5 seborrheic keratoses. Note the higher intensity of the green channel compared to melanomas.

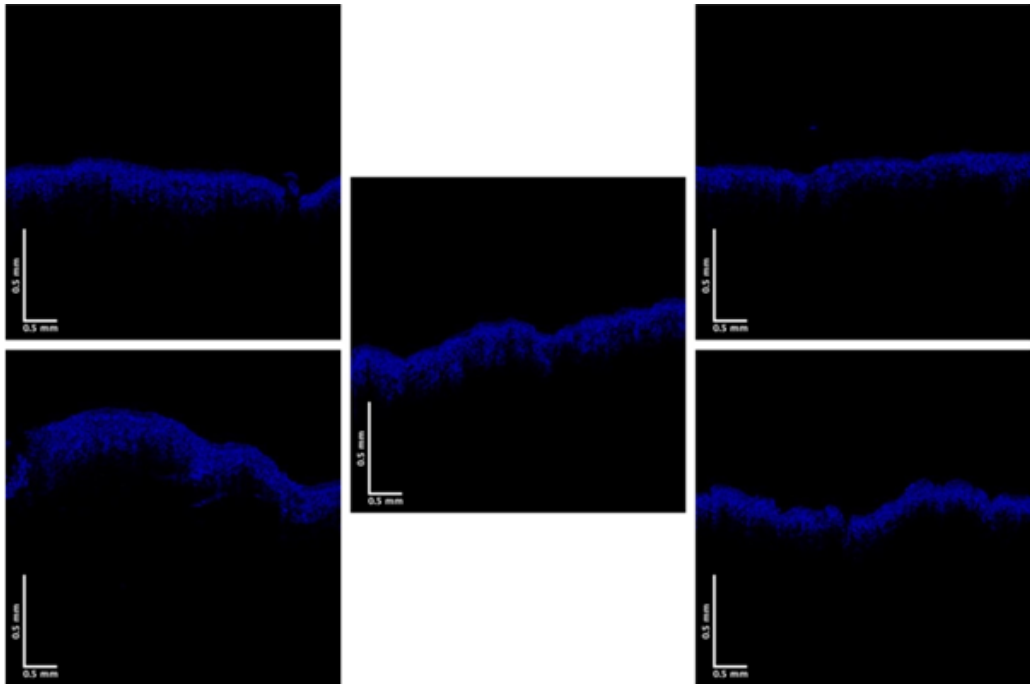

Figure 9: Blue channel OCT images of 5 melanomas.

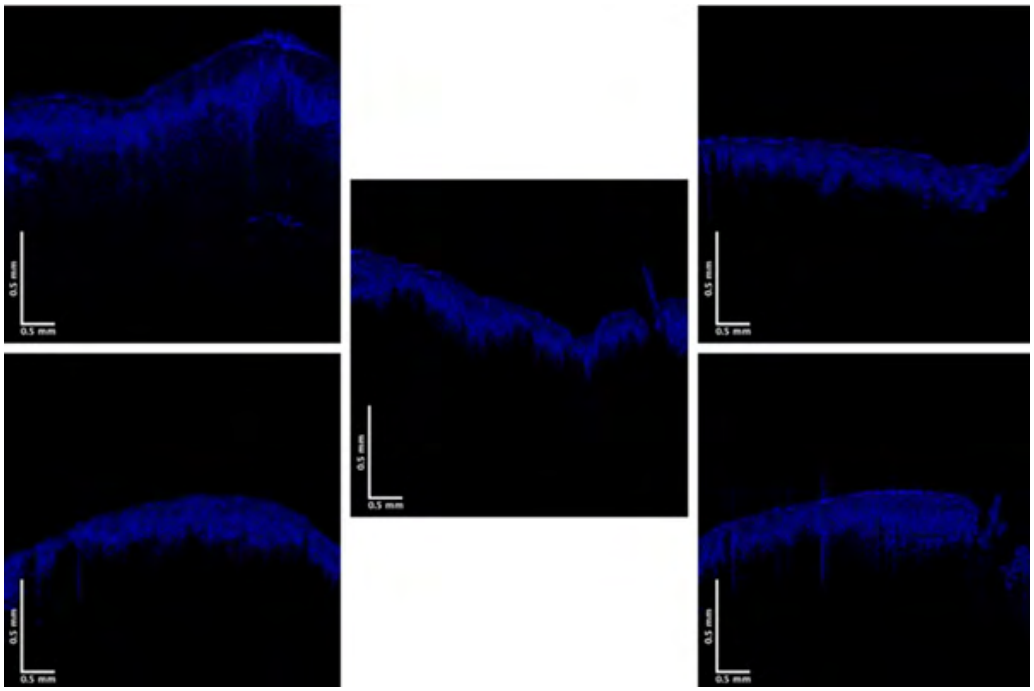

Figure 10: Blue channel OCT images for 5 seborrheic keratoses.

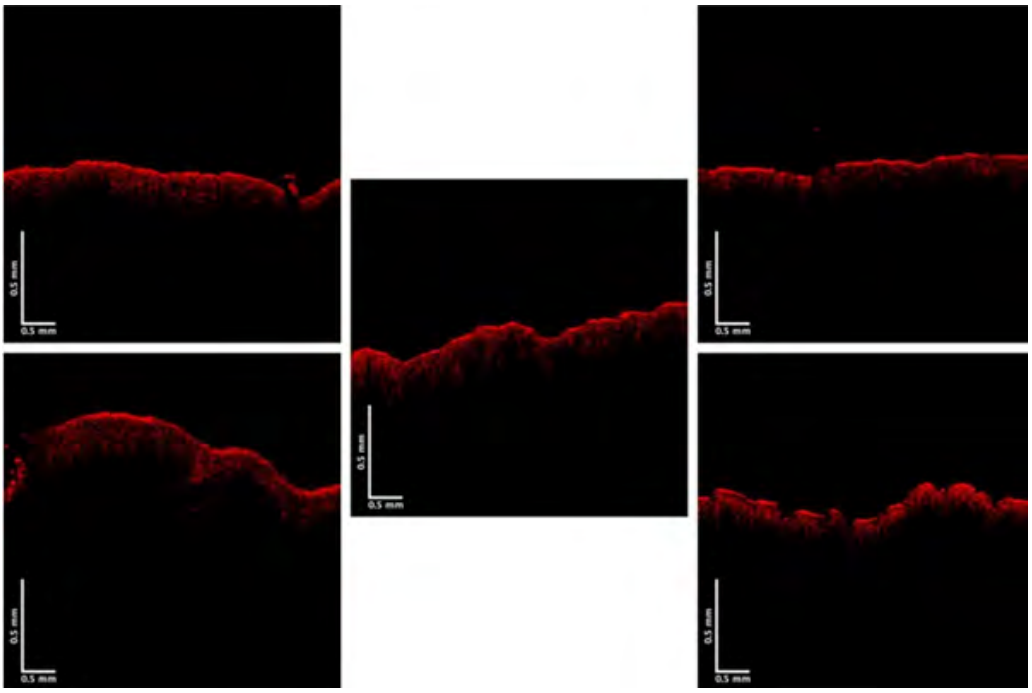

Figure 11: Red channel OCT images for 5 melanomas.

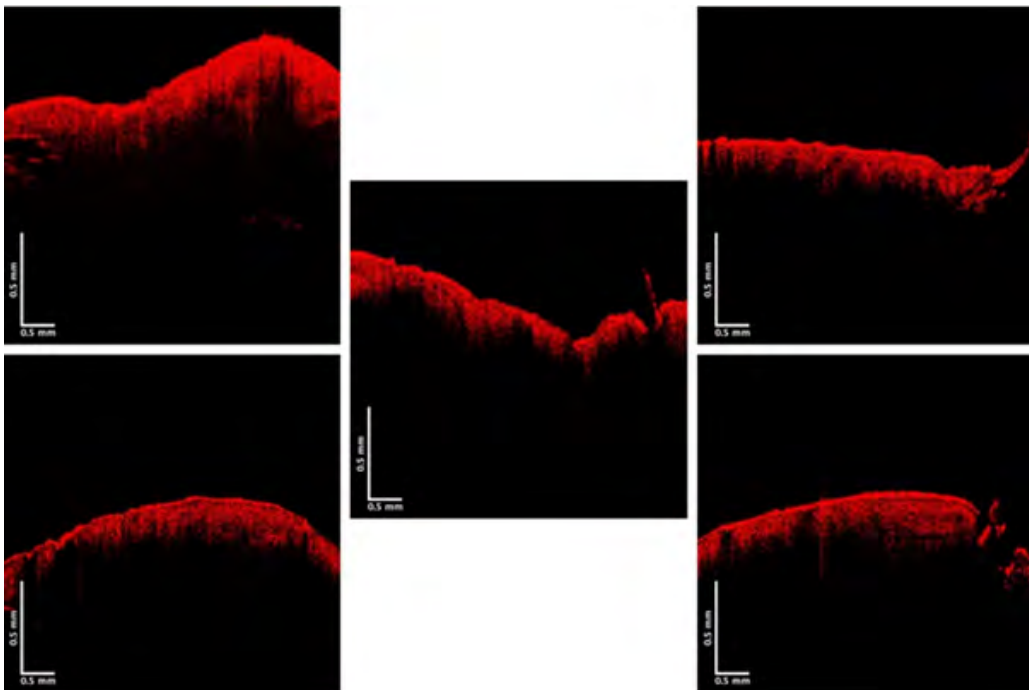

Figure 12: Red channel OCT images for 5 seborrheic keratoses. Note the higher pixel intensity of SKs compared to melanomas.

Table 1: Fire Lookup Table (LUT) for color coding the OCT images.

Greyscale value	Red Channel	Green Channel	Blue Channel
0	0	0	0
50	104	0	221
100	201	7	78
150	255	129	0
200	255	219	0
255	255	255	255

5. Discussion

The objective of this pilot study is to illustrate that OCT images of skin lesions are rich in information that can be used to noninvasively to differentiate between OCT images of normal skin, BCC, SCC, SK and melanomas. It is also possible to identify differences between benign pigmented lesions (SK) and pigmented melanomas. While OCT research has been reported to evaluate pathological skin conditions [2, 4, 5, 8-12] additional details can be gleaned beyond just examining OCT images by eye. It is possible to use OCT images to evaluate differences among skin lesions by producing images using the pixel intensity as a function of depth from pixel intensity measurements [12, 21]. The ability to create pixel density images from OCT images using green, blue, and red colors to represent the distribution of pixels yields additional information that can be evaluated in different skin conditions. The results presented in Figures 1 and 2 suggest that there are differences among normal skin, BCC, SCC, and melanoma when comparing mages based on pixel intensity distribution. Since there is little absorption by skin chromophores at light wavelengths between 600 and 1000 nm, the differences observed in this pilot study at 840 nm are likely to be a result of scattering differences especially by SCC and melanoma (Figure 2). The enhanced scattering by SCC and melanoma may be due to the formation of elements in the epidermis that are greater than 1/10 the wavelength of light which are larger than those scattering units in normal skin and BCC. Since Mie scattering occurs in the forward direction, the decreased pixel intensities in SCC and MEL are likely to reflect the formation of aggregates of cells, small blood vessels, melanin particles and/or deposition of fibrous collagen in the epidermis. These may be aggregates of cells, but in the case of melanoma it may reflect the formation of large accumulations of melanin particles. Recently it was reported that melanin stacking differences may occur in highly pigmented melanomas based on OCT images and vibrational optical coherence tomography measurements [12]. These stacking differences may reflect differences in melanin type as well as interparticle forces. Two forms of melanin are produced in skin, yellow-red pheomelanin and black-brown eumelanin [19,22-24]. Eumelanin that is present in skin contributes to darker skin color compared to pheomelanin. Eumelanin is thought to be effective in absorbing UV light. Scattering properties of skin are due to the presence of

melanin and melanosomes, specialized organelles within cells that produce, store, and transport melanin [19, 22-25]. Cutaneous malignant melanomas often exhibit pigmented regions that are darker than the surrounding skin. While melanoma cells are the original source of melanin, keratinocytes, and melanophages (macrophages containing melanin) also contribute to the tumor color because they contain melanin obtained from melanoma cells [25, 26]. Scattering from melanosomes and fragmented melanosomes is of particular significance [25]. Melanin particles are particularly good scatterers since they have very high refractive indices and are contained within melanosome particles of dimensions up to 1000 nm in size. Cutaneous malignant melanomas often exhibit pigmented regions that are darker than the surrounding skin. Corneal and epidermal layers in skin forward scatter light to deeper skin layers due to keratin orientation and Mie scattering by organelles and melanosomes [26]. Melanosomes are formed in melanocytes but are transferred to the keratinocytes. As the keratinocytes move upward in the skin, they become fragmented (26). Large melanin particles scatter light forward towards the papillary dermis. Collagen fibers in the papillary dermis are small and result in Raleigh scattering of light in all directions while large collagen fibers of the reticular dermis result in Mie scattering in the forward scattering direction [27]. Therefore, forward scattering of infrared light by large cell aggregates and melanin particles in the epidermis results in increased pixel intensity in the images of the lower epidermis. In comparison, the pixel intensity is decreased in the red channel of melanomas due to further forward Mie scattering into the rectangular dermis that is not seen in the images. The increased green pixel intensity images of SK lesions compared to melanomas suggests that the melanin particle size is much smaller in SK lesions. Quantifying the green, blue, and red channels that are derived from OCT scanned images of skin may be a noninvasive method to screen patients at risk for developing melanoma. Patients with red hair have mutations in the MC1R gene causing its inactivation; this leads to a paucity of eumelanin production and makes redheads more susceptible to skin cancer including melanoma [28]. The mechanism by which pheomelanin promotes carcinogenesis may be related to increased ROS (reactive oxygen species) production that is associated with its synthesis [28]. Eumelanin is UV light absorbent, whereas pheomelanin, is photounstable and may even promote carcinogenesis [28]. Pheomelanin melanosomes are generally small and oval, in contrast to the larger elongated shape of eumelanin containing melanosome [28]. If eumelanin forms large particles in melanoma, then this would explain why the green channel image for melanoma is weaker than for the other lesions tested. The results of this pilot study suggest that further work is needed to determine if lesion type can be accurately determined based on additional quantitative analysis of pixel intensity profiles.

6. Conclusions

We have studied the pixel intensity profiles of OCT images of normal skin, basal cell carcinoma, squamous cell carcinoma, seborrheic keratosis, and melanoma by breaking OCT images into low (green), medium (blue) and high (red) pixel intensity OCT images. While normal skin, seborrheic keratosis, and basal cell carcinoma are characterized by higher green scale pixel intensity images, squamous cell carcinoma and melanoma have lower green scale pixel intensity images. Melanoma has a lower red scale pixel intensity versus depth compared to the other lesions. Our results show decreased pixel intensity of SCC and melanomas is likely due to formation of cellular and melanin aggregates that approach the wavelength of light in size. The decreased pixel intensity of melanoma appears to be a result of increased amounts of large cellular aggregates and melanin particles in melanocytes, keratinocytes and macrophages. Quantitative pixel intensity measurements may be useful to identify cancerous lesions in patients that may be predisposed to SCC and melanoma; however, further study results are needed.

References

1. Park ES. Skin-Layer Analysis Using Optical Coherence Tomography (OCT) Med Lasers. 2014; 3(1): 1-4.
2. Olsen J, Holmes J, Jemec GB. Advances in optical coherence tomography in dermatology-a review. J Biomed Opt. 2018; 23(4): 1-10.
3. Zeppiei M, Marsili S, Enaholo ES, Shuaibu AO, Uwagboe N, Salati C. Optical Coherence Tomography (OCT): A Brief Look at the Uses and Technological Evolution of Ophthalmology. Medicina. 2023; 59: 2114.
4. Wan B, Ganier C, Du-Harpur X, Harun N, Watt FM, Patalay R. Applications and future directions for optical coherence tomography in dermatology. British Journal of Dermatology. 2021; 184: 1014-1022.
5. Mogensen M, Thrane L, Jørgensen TM, Andersen PE, Jemec GB. OCT imaging of skin cancer and other dermatological diseases. J Biophotonics. 2009; 2(6-7): 442-51.
6. Jung SE, Kang HY, Lee ES, Kim YC. Changes of epidermal thickness in vitiligo. Am. J. Dermatopathol. 2015; 37 (4): 289-292.
7. Chao CY, Zheng YP, Cheing GL. Epidermal thickness and biomechanical properties of plantar tissues in diabetic foot. Ultrasound Med. Biol. 2011; 37: 1029-1038.
8. Baran U. High resolution imaging of acne lesion development and scarring in human facial skin using oct-based microangiography. Lasers Surg. Med. 2015; 47(3): 231-238.
9. Deegan, Anthony J, Faezeh Talebi-Liasi, Shaozhen Song, Yuandong Li. Flowers, Stephanie J. Lee, and Ruikang K. Wang. Optical coherence tomography angiography of normal skin and inflammatory dermatologic conditions. Lasers in surgery and medicine. 2018; 50 (3): 183-193.
10. Babalola O, Mamalis A, Lev-Tov H, Jagdeo J. Optical coherence tomography (OCT) of collagen in normal skin and skin fibrosis. Arch Dermatol Res. 2014; 306(1): 1-9.
11. Sattler E, Kästle R, Welzel J. Optical coherence tomography in dermatology. J Biomed Opt. 2013; 18(6): 061224.

12. Silver FH, Deshmukh T, Nadiminti H, Tan I. Melanin Differences in Pigmented and Non-Pigmented Melanomas: Quantitative Differentiation between Pigmented and Non-Pigmented Melanomas Based on Light-Scattering Properties. Life. 2023; 13: 1004.
13. Lister T, Wright PA, Chappell PH. Optical properties of human skin. J Biomed Opt. 2012; 17(9): 90901-1.
14. Jacques SL. Optical properties of biological tissues: a review. Physics in Medicine & Biology. 2013; 58(11): R37.
15. Yang MF, Tuchin VV, Yaroslavsky AN. Principles of light-skin interactions. In: Light-Based Therapies for Skin of Color. Springer. 2009; 1-44.
16. Diffey BL. What is light? Photodermatology, photoimmunology & photomedicine. 2002; 18(2): 68-74.
17. Zonios G, Dimou A, Bassukas I, Galaris D, Tsolakidis A, Kaxiras E. Melanin absorption spectroscopy: new method for noninvasive skin investigation and melanoma detection. Journal of biomedical optics. 2008; 13(1): 014017.
18. Xiao M, Chen W, Li W. Elucidation of the hierarchical structure of natural eumelanins. Journal of The Royal Society Interface. 2018; 15(140): 20180045.
19. Illina A, Thorn KE, Horn PA, Wagner I, Tamming R, Sutton JJ. The photoprotection mechanism in the black–brown pigment eumelanin. Biophys Comp Biol. 2022; 119(4): 22212343119.
20. Nasti TH, Timares L. MC1R, eumelanin and pheomelanin: their role in determining the susceptibility to skin cancer. Photochem Photobiol. 2015; 91(1): 188-200.
21. Silver FH, Deshmukh T, Nadiminti H. Melanin Stacking Differences in Pigmented and Non-Pigmented Melanomas: Quantitative Differentiation between Pigmented and Non-Pigmented Melanomas Based on Light-Scattering Properties. Life. 2023; 13: 1004.
22. Micillo R, Panzella L, Koike K, Monfrecola G, Napolitano A, d'Ischia M. "Fifty Shades" of Black and Red or How Carboxyl Groups Fine Tune Eumelanin and Pheomelanin Properties. International journal of molecular sciences. 2016; 17(5): 746.
23. Hunt G, Kyne S, Ito S, Wakamatsu K, Todd C, Thody AJ. Eumelanin and pheomelanin contents of human epidermis and cultured melanocytes. Pigment cell research. 1995; 8(4): 202-208.
24. Nielsen KP, Zhao L, Juzenas P, Stamnes JJ, Stamnes K, Moan J. Reflectance Spectra of Pigmented and Nonpigmented Skin in the UV Spectral Region† Photochemistry and Photobiology. 2004; 80(3): 450-455.
25. Zonios G, Dimou A. Light scattering spectroscopy of human skin in vivo. Opt Express. 2009; 17(3): 1256-67.
26. Bruls WAG, Van der Luen JC. Forward scattering properties of human epidermal layers. Photochem. Photobiol. 1984; 40: 231-242.
27. Gajinov Z, Mati M, PrĆiĆ S, Duran V. Optical properties of the human skin. Serbian Journal of Dermatology and Venereology. 2010; 2 (4): 131-136.
28. Nasti TH, Timares L. Invited Review MC1R, Eumelanin and Pheomelanin: their role in determining the susceptibility to skin cancer. Photochem Photobiol. 2015; 91(1): 188-200.